SATTELITE DESIGN PROJECT

Final Design Report

Ahmed Moussa

Stu. No: 101142994
ahmedamoussa@cmail.carleton.ca

AERO3841 – Spacecraft Design I
2024-04-09

Table of Contents

1 – Introduction

This mission's goal is to quantify the burned areas of Earth's boreal forest using satellite imaging. Data sourced from the satellite's images can support sustainable management of Earth's forests and may be used to quantify greenhouse gasses such as carbon dioxide and monoxide released by burned forest. The mission can also be extended to monitor freshwater reserves and the macro effects of climate change on the ecosystem.

The satellite must capture images of the entire boreal forest within 14 days. The image resolution must be 100m x 100m. A cylindrical payload camera is provided by the customer. Its details can be found in Table 1.1. The satellite will communicate with the Gatineau Satellite Ground Station to transfer images and receive commands.

TABLE 1.1 – Fixed Mission Requirements & Parameters

Requirement/Parameter	Value
Max Imaging Cycle Time	14 days
Camera FOV	20°
Camera Diameter	0.5m
Camera Length	0.5m
Camera Power Rating	300 W
Camera Mass	250 kg
Resolution	100m x 100m

See Appendix A for the project schedule and Appendix B for the cost estimates.

2 – Orbit Selection

A circular low-earth orbit (LEO) is selected since the desired image resolution is relatively fine at 0.01 km^2. A much more expensive telescopic payload hosting large and heavy lenses would be required to meet the requirement at higher altitudes. Since the boreal forest is mainly situated between the latitudes of 50^0 and 70^0 [1], the circular orbit's inclination is set to 70°.

The orbit's design is constrained by two fixed parameters in Table I. Firstly, the maximum imaging cycle time is used to minimize the data (image size) captured per orbit. Secondly, the camera FOV designates how large is the area captured per image. The radius of the camera's capture area is estimated using Eq. 2.1. For simplicity of this preliminary design, the curvature of the Earth is not considered when estimating the capture area.

$$R_{FOV} = H \times tan\frac{\theta_{FOV}}{2} \tag{2.1}$$

Square-shaped images are processed to avoid gaps and to optimize the capture and data rates. To minimize gaps with circular images, an increased capture rate is needed as illustrated in Fig. 2.1. On the contrary, square-shaped images enable the satellite to flawlessly capture a grid of images without gaps and at the lowest capture rate. The image side-length is represented by Eq. 2.2. See Fig. D1 for an overview of the geometric analysis.

$$x = \sqrt{2}\, R_{FOV} = H\sqrt{2}\, tan\frac{\theta_{FOV}}{2} \tag{2.2}$$

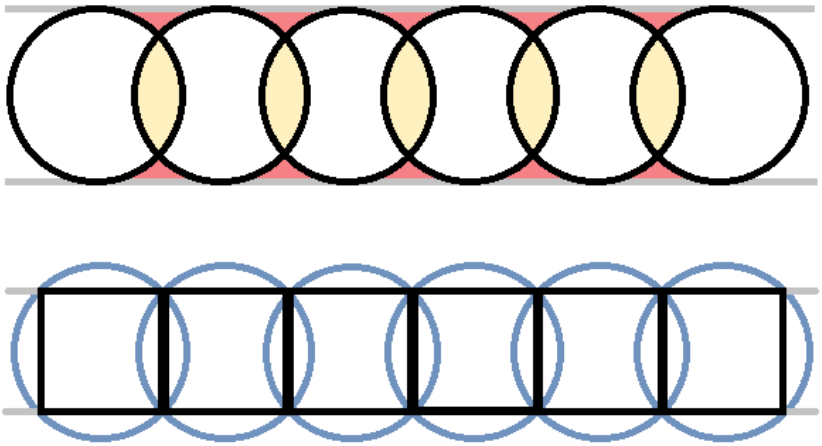

Figure 2.1 – Circular image captures vs. square image captures. Gaps between images are highlighted in red. Overlap between images are highlighted in yellow.

During the operation of this satellite, its ground tracks will regress around along Earth's longitude. Once the ground tracks have regressed a full 360°, there will be a longitudinal overshoot between the initial ground track of the first cycle and the second cycle and so forth. If the nodal precession (i.e. ground track's longitude shift per orbit) is a value that results in an overshoot equivalent to the longitudinal ground coverage of the payload, the onboard camera will be exposed to the entirety of the globe over time with maximized efficiency.

TABLE 2.1 - Orbit Altitude Iterative Solution

Altitude [km]	Coverage [deg]	Nodal Precession [deg]	Excess Precession [deg]
800	1.7941	25.2479	6.5289
850	1.9062	25.5125	2.8256
860	1.9286	25.5655	2.0834
862	1.9331	25.5761	1.9349
862.0228	1.9332	25.5762	1.9332

Assuming that the total precession overshoot is equivalent to the longitudinal ground coverage per image, the altitude needed to match the two values can be solved iteratively as shown in Table 2.1. This altitude estimate does not consider J2 orbit perturbation among other effects such as atmospheric drag. When the orbit is simulated and refined using STK software, an ideal altitude of 830.15 km is observed. The ground tracks over 14 days are plotted in Fig. D2. Furthermore, via STK it is observed that a right ascension of the ascending node (RAAN) of 240° ensures that the boreal forest is always in daylight time when photographed. See Table 2.2 for an overview of the orbit's properties and parameters.

TABLE 2.2 - Orbit Properties & Parameters

Inclination	70°
Eccentricity	0
RAAN	240°
Radius (Semimajor Axis)	7201.15 km
Period	6081.55 s
Speed	7.4399 km/s
Orbits per Day	14.21
Ground Station Access Time	612.52 s

3 – Spacecraft Bus

3.1 – Mass & Power Budgets

TABLE 3.1 – Preliminary Mass Budget Estimate

Subsystem(s)	Mass [kg]	%	Justification
Payload	250	50	Requirement.
Structure	75	15	A lightweight structure is ideal for a small LEO satellite.
Thermal	25	5	Standard passive thermal control.
Power	100	20	Solar panels and a power supply system are needed on the satellite. This value will be further refined once the solar panel criteria and characteristics are finalized.
TT&C + C&DH	25	5	Along with the circuitry involved, an antenna as well as a beam steering mechanism need to be included in the communications subsystem.
ADCS + G&N	10	2	Attitude control mechanisms on this satellite do not need to be capable of performing frequent large angle maneuvers. The satellite's mass is also assumed to be distributed in a fashion that makes stabilization easy (axisymmetric).
Propulsion	15	3	A small propulsion system needs to be integrated for initial orbit insertion and satellite decommissioning.
Dry Mass	500	100	
Dry Mass + Margin (30%)	650	130	
Fuel Mass*	45.47	--	
TOTAL	695.47	--	

* See Section 3.7 for ΔV and fuel mass estimates.

TABLE 3.2 – Preliminary Power Budget Estimate

Subsystem(s)	Power [W]	%	Justification
Payload	300	60	Requirement.
Structure	0	0	There is no need for electromechanical parts on the structure. Antenna steering is included in TT&C.
Thermal	0	0	Passive thermal control techniques are suitable.
Power	75	15	Power generation, storage, and distribution systems. Power management systems also need to operate since the payload consumes 300W during both daylight & eclipse conditions.
TT&C + C&DH	75	15	A good amount of power is needed for the X-band antenna used to deliver high-resolution images. Furthermore, the antenna is a mechanically steered reflector antenna which consumes power to steer the beam transmission or reception direction.
ADCS + G&N	37.5	7.5	Nadir-pointing passive attitude control techniques (gravity gradient) reduce the amount of power needed for ADCS. G&N requires a moderate amount of power to determine the satellite's precise location to provide image metadata that also enables the images to be indexed and/or stitched.
Propulsion	12.5	2.5	Power for the propulsion system during initial orbit correction and the decommissioning maneuver. It is on the lower end since the propulsion time and precision needed to make such maneuvers in orbit is very small.
TOTAL	500	100	
TOTAL + Margin (10%)	550	110	

TABLE 3.3 – Revised Preliminary Power Budget Estimate

Subsystem(s)	Power [W]	%	Justification
Payload	300	70	Increased due to the net decrease of other subsystem power requirements.
Structure	0	0	--
Thermal	32.14	7.5	Increased due to addition of a 30W resistive heater.
Power	32.14	7.5	Decreased since power management system is simple for this consistent mission and simple payload.
TT&C + C&DH	21.43	5	Decreased since transmit power is much smaller than initially anticipated (see Section 3.2.2).
ADCS + G&N	32.14	7.5	--
Propulsion	10.71	2.5	--
TOTAL	428.57	100	
TOTAL + Margin (10%)	471.43	110	

3.2 – Communications

3.2.1 – DATA BUDGET & RATES

ASSUMPTIONS

Access Time per Day: 612.52 s/day
Boreal Forest Area: 12 million km^2
Uplink Bitrate: 1000 bps
Data Compression: 4x
Telemetry Sampling Rate: 100/min or 144000/day
Telemetry Sample Size: 16 bits

Having the satellite orbit defined, it is possible to determine what data transfer rates are needed for the downlink and uplink. To do so, the ground coverage of the payload camera must be analyzed. See Fig. 3.1 for the calculation of the ground coverage.

Ground Coverage

$FOV_{cam} = 20^o$
$H_{orbit} = 830.15$ km

$D_{FOV} = 2H_{orbit}\sin\left(\frac{FOV_{cam}}{2\sqrt{2}}\right) = 204.38$ km
$A_{FOV} = D_{square}^2 = 41772.63$ km^2

Access Time
$t_{down} = 0.8 \times 612.52 = 490.016$ s
$t_{up} = 0.2 \times 612.52 = 122.504$ s

Data Budget

Resolution = 0.01 km^2

$PX_{img} = A_{FOV}/0.01 = 4.18 \times 10^6$ px
$PX_{total} = 4 \times PX_{img} = 1.67 \times 10^8$px
$Size = 16 \times PX_{total} = 2.67 \times 10^8$ bits = 254.96 Mbits

$A_{day} = \frac{12\times10^6 \text{ km}^2}{14 \text{ days}} = 857'142.86$ km^2/day
Daily Image Rate $= \text{ceil}\left(\frac{A_{day}}{A_{FOV}}\right) = 21$ img/day
Daily Image Bit Rate = 5.61×10^9 bits/day

Data Rates

$R_{img} = \frac{5.61\times10^9 \frac{\text{bits}}{\text{day}}}{4t_{down}} = 2.86 \times 10^6$ bps $= 2.73$ Mbps
$R_{misc} = \left[21 \text{ img} \times (32+32+32+64+24) + 3 \times \frac{5.61\times10^9 \text{bits}}{8\text{bits/byte}}\right]/4t_{down} = 1.07 \times 10^6$ bps $= 1.02$Mbps
$R_{tele} = \frac{144000\ samples \times 16 \text{ bits}}{4t_{down}} = 1175.47$ bps $= 0.001$ Mbps
$R_{total} \cong 3.75$ Mbps

Figure 3.1 – Calculations for ground coverage, data budget per day, and data transfer rates.

Provided with a desired resolution of 100m x 100m (0.01 km^2), the number of bits per image is computed to be 2.67×10^8 bits. Each pixel contains 4 channels of data for RGB and infrared which each contain 16 bits of data per channel. The image data transfer per day sums up to 5.61×10^9 bits/day for 21 images. To transfer this much data with an estimated downlink access time of 490.02 s, a transfer rate of at least 2.73 Mbps is needed. Each image taken also includes metadata containing its latitude, longitude, altitude, time, synchronization, and error tracing. This metadata costs up to 1.02 Mbps in downlink throughput according to the calculations in Fig. 3.1. In total, the downlink needs approximately 3.75 Mbps of downlink throughput to effectively meet the mission objectives. As a safety precaution for when the link is briefly unavailable and for the small remainder of bps needed beyond 3.75 Mbps, the design downlink is extended to 4.00 Mbps.

3.2.2 – LINK BUDGET

ASSUMPTIONS

Bit-Error-Rate (BER): 10^{-5}
Downlink Noise Temperature: 300 °K
Uplink Noise Temperature: 100 °K
Spacecraft Antenna Diameter: 0.2m
Downlink Elevation: 10°
TX/RX Efficiency: 0.65

Due to the high-resolution of the images captured by the payload, an X-band downlink antenna operating at 8.2GHz is selected for the preliminary design. Frequencies in the X-band are also less susceptible to rain fade. For this preliminary design analysis, a fade margin of 15 dB for 99% link availability is considered [2]. The selected frequency is compatible with the Gatineau ground station which hosts both S & X band capabilities using 13-meter reflector antennas [3]. Of the TT&C + C&DH power budget, this preliminary design will assume that 75% of the allocated subsystem power is used for transmit power; hence 75W.

To determine the satellite antenna's gain and dimensions, the achieved signal-to-noise ratio (SNR) for the modulated signal must be determined. The required SNR for a Quadrature Phase Shift Keying (QPSK) modulated signal for the desired BER and bitrate is computed in Fig. 3.2 below. Adding the fade margin to the required SNR yields the achieved SNR which is equal to 33.03 dB.

Required & Achieved SNR

BER = 10^{-5}
F.M = 15 dB
R = 4 Mbps = 4'194'304 bps
B = 0.6 x R = 2516582.40 Hz = 2.5166 MHz

$$\left(\frac{S}{N}\right)_{req} = \frac{R}{B}\ln\left(\frac{1}{2\text{BER}}\right) = \frac{10000}{6000}\ln\left(\frac{1}{2\times10^{-5}}\right) = 18.03 \text{ dB}$$

$$\left(\frac{S}{N}\right)_{\text{ach}} = \left(\frac{S}{N}\right)_{\text{req}} + \text{F.M.} = 33.03 \text{ dB}$$

Wavelength

$$\lambda = \frac{c}{f} = 0.03659 \text{ m}$$

Gains

D_r = 13m D_t = 0.2m
η_r = 0.65 η_t = 0.65

$$G_r = 10\log\left[\eta_r\left(\frac{\pi D_r}{\lambda}\right)^2\right] = 59.0849 \text{ dB}$$

$$G_t = 10\log\left[\eta_t\left(\frac{\pi D_t}{\lambda}\right)^2\right] = 22.8266 \text{ dB}$$

Transmit Power

R_E = 6371 km h = 830.15 km
δ = 10°

$$d = R_E \times \left(\sqrt{\left(\frac{R_E+h}{R_E}\right)^2 - \cos^2\delta} - sin\delta\right) = 2427926.807 \text{ m}$$

$$\left(\frac{S}{N}\right)_{\text{ach}} = P_t + G_t + G_r + 20\log\frac{\lambda}{4\pi d} - 10\log kTB \text{ [dB]}$$

$$\boldsymbol{P_t = 33.03 - 59.0849 - 22.8266} + 10\log[k(300)(2.517\times10^6)] - 20\log\frac{\lambda}{4\pi d} = -10.28 \text{ dBW} = 0.094 \text{ W}$$

Figure 3.2 – Calculations for the achieved SNR, antenna gains, and transmit power.

The Gatineau satellite station's antenna is estimated to have a gain of 59.08 dB while assuming an efficiency of 0.65. Making an assumption that the satellite antenna aperture diameter is 0.2m enables the computation of the transmission gain 22.83 dB. These gains seem reasonable. When the SNR link budget equation is used to solve for the transmission power, the resulting value of -10.28 dBW or 0.094W. From this it is evident that the 75W of budgeted power is completely unnecessary. TT&C + C&DH budgeted power is reduced significantly in the revised final power budget seen in Table 3.3.

3.3 – Power

The mission requirements state that the payload must be operational throughout the entire orbit. Consequently, batteries are needed to provide power during orbital eclipse time. When exposed to solar radiation, solar cells must provide sufficient energy to power the satellite and charge the batteries for the oncoming eclipse cycle. Direct energy transfer (DET) power regulation is implemented since it is simple and capable of dissipating useful heat to the thermal subsystem (further explained in Section 3.6).

3.3.1 – ECLIPSE TIME

Worst case eclipse time is calculated by assuming the Earth is spherical and its shadow is a perfect cylinder as illustrated in Fig. D3. In practice, the sun's light refracts through the atmosphere and is partially visible during some regions of the eclipsed cylinder. Computations seen in Fig. C1 yield a maximum eclipse time of 35.03 minutes which is 34.57% of this mission's orbital period.

3.3.2 – SOLAR PANELS

Solar panels consisting of gallium arsenide (GaAs) were selected due to their high availability for spacecraft applications and reasonably high efficiency of 244.4 W/m^2 during worst-case solar irradiance [4]. With DET power regulation, the path efficiency of the solar array output is approximately 0.65 during eclipse time and 0.85 during daylight time [4]. Given these efficiencies, Eq. 3.1 can be used to compute a solar power production requirement of 937.74 W.

$$\mathrm{P_{sa}} = \frac{\frac{PT_e}{X_e} + \frac{PT_d}{X_d}}{T_d} \tag{3.1}$$

Following the computations performed in Fig. C2, the solar array's BOL and EOL power densities are 172.57 W/m^2 and 142.55 W/m^2 respectively. For the specified EOL power density, a solar array area of 6.58 m^2 is needed to produce the required power. Details on solar array geometry and placement can be found in Section 11. Assuming a mass ratio of 25 W/kg, the total solar array mass is estimated to be 34.1kg which is well within the power subsystem initial mass budget allocation of 100 kg. The mass ratio 25 W/kg is a conservative estimate for solar panels since it can extend up to 100 W/kg and beyond [4].

3.3.3 – BATTERY SIZING

Considering the satellite orbits Earth 14.21 times per day, the satellite batteries will experience 5186.65 charge/discharge cycles per year. Throughout the 5-year mission life, approximately 25'933 cycles occur. Lithium-ion batteries have been increasingly used on satellite missions due to their high specific energy of 90+ Wh/kg and BOL depth-of-discharge (DOD) of around 80% [5]. After 25'993 charge/discharge cycles, an Li-ion battery has a DOD of 25% which is an improvement relative to the 20% DOD a NiCd battery offers [5][6].

Four batteries are used for redundancy. Computations shown in Fig. C3 demonstrate that each battery needs a charge capacity of 316.56 Wh. Considering the worst-case Li-Ion battery (90 Wh/kg), each battery has a mass of 3.52 kg. The total mass of all four batteries is 14.07 kg which is well below the allocated power subsystem's initial mass budget allocation.

3.3.4 – BUS & HARNESS DESIGN

The satellite modest bus voltage of 24V because of its small size and relatively low power rating [4]. Since Li-Ion batteries tend to maintain a consistent voltage throughout the majority of their charge; an unregulated bus is selected for this mission. Considering the satellite isn't too large and has much of its circuitry stacked in a modular fashion (see Section 4), the power harness mass should only account for 10kg (10%) of the power subsystem's mass. A loss of up to 47.14 W (5%) can be attributed to the cabling and connections [4]; however, this is totally acceptable since there is a 10% margin included in the revised power budget (Table 3.3).

3.4 – Attitude Control

Mission requirements include a 1° attitude control accuracy and a 0.1° attitude determination accuracy. Reaction wheels paired with gyroscopes and sun sensors can deliver this level accuracy under the influence of a PD or dynamic adaptive controller.

Four reaction wheels are used for the attitude control of this satellite. Three of the reaction wheels are aligned with each of the body's primary axes. For redundancy, a fourth reaction wheel is aligned in a fashion where it can influence all three axes. Reaction wheels apply internal torques to counter attitude perturbations and maintain a satellite orientation. Pertinent perturbations are the interference with Earth's magnetic field, solar radiation pressure torque, and a gravity gradient torque caused by Earth's gravitational field trying to align the satellite's major axis of inertia with the Earth's normal. This alignment is known as the nadir-pointing orientation. Due to this satellite's small dimensions, the gravity gradient torque is insufficient to maintain this orientation.

To maintain a nadir-pointing orientation such that the payload camera is always aligned with the Earth's normal, a reaction wheel actively rotates the satellite about the yaw axis with a rotation rate equivalent to the orbital angular velocity. As the yaw wheel rotates, it accumulates angular momentum which may reach a saturation point leading to a control failure. A magnetorquer is used to dump this excess angular momentum via interaction with Earth's magnetic field. The magnetorquer can also be used as a backup attitude control mechanism. Besides counteracting attitude perturbations and maintaining an orientation, the reaction wheels are also needed to perform large maneuvers to orient the satellite post-deployment.

A gyroscope is used to measure the rate of change in attitude across all axes. Two sun sensors on opposing sides of the satellite and one on the top face are needed to determine the roll, pitch, and yaw. Knowing the true anomaly of the satellite, the light intensity received by the sun sensors can be estimated and compared with the measured data to make attitude estimates and corrections. The satellite's pitch can also be calibrated based on the images taken by the payload.

3.5 – Guidance & Navigation

Initial orbit injection/adjustment and the de-orbiting maneuver are the only G&N operations of this mission. Perturbations affecting the satellite's orbit include atmospheric drag, gravitational perturbations, and solar radiation effects. At the relatively high 830km LEO altitude, the atmosphere is very thin hence the atmospheric

drag is negligible [7]. Solar radiation pressure against the satellite is also comparably small on the scale of 10^{-7} m/s^2 [7]. The gravitational pull of the moon and sun have a slightly greater influence on the scale of 10^{-6} m/s^2 [7]. The most relevant orbital perturbation affecting this mission is the J2 perturbation caused by the oblateness of the Earth. The high inclination of the orbit also implies a stronger J2 influence since the gradient of the Earth's radius is steeper.

3.5.1 – ORBIT CONTROL STRATEGY

Orbit maintenance is not needed since the optimized mission altitude of 830.15km considers all these perturbations. There is also some overlap between photos taken which can cover any miniscule offsets caused by orbital imperfections. Due to the simple and passive nature of this mission, autonomous control is sufficient to operate the satellite. Ground control for emergency situations such as physical damage or software faults is desirable to maintain the mission realiability for as long as needed. Parameters revolving around heater and propellant control such as heater power and propellant massflow should be considered for ground control.

3.5.2 – DE-ORBITING STRATEGY

To de-orbit the satellite at the end-of-life, small thrusters are engaged with the remaining propellant to reduce the orbit altitude to 600km. At this altitude, atmospheric drag will de-orbit the spacecraft over the duration of 25 years [8]. If the mass budget allows for it, more propellant can be used to bring the satellite down to sub-400km altitudes where it will de-orbit within a year [8].

3.6 – Thermal Control Subsystem

The mission requirements specify a maximum and minimum spacecraft temperature of 50°C and -5°C respectively. A safety margin of 5°C is also requested. The payload has a sensitive operating temperature of 20±1°C. For preliminary design estimates, the spacecraft is assumed to be an isothermal sphere. A sphere has the minimum surface area for a given volume, thus it minimizes the emission surface and consequently represents the worst-case scenario for thermal control. The objective is to satisfy the ideal equilibrium temperature range of 0-45°C using passive thermal control which is simpler and cheaper than active control.

3.6.1 – THERMAL BALANCE

Radiation from the Sun and Earth as well as the reflected albedo energy from Earth are all considered in the thermal analysis. Given an isothermal spherical satellite, Eq. 3.2 represents the energy balance between its thermal emissions and absorbed plus generated thermal energy.

$$G_s \frac{A_{sc}}{4} \alpha_s + \dot{q}_E \sin^2(\rho) A_{sc} \frac{1 - cos\,\rho}{2} + G_s A_{sc} a \alpha_s \frac{1 - cos\,\rho}{2} \sin^2(\rho) + \dot{Q}_W = \varepsilon_{IR} A_{sc} \sigma T^4 \qquad (3.2)$$

In Eq. 3.2, ρ represents the Earth angular radius, A_{sc} is the total surface area of the spacecraft, G_s is the solar irradiance constant, $\dot{q}_E$ is Earth's IR heat flux (237±21 W/m^2), a is Earth's albedo (30±5%), α_s is the solar absorptivity of the spacecraft, $\dot{Q}_W$ is the spacecraft power generation, ε_{IR} is the spacecraft's IR emissivity, and σ is the Stefan-Boltzmann constant (5.67 x 10^{-8} W/m^{2}K^4). The Earth's angular radius is resolved in Fig. D4.

3.6.2 – WORST CASE CONDITIONS

Initial estimates are made using the initial preliminary power budget. For a worst-case cold (WCC) condition during total eclipse, the only thermal energy absorbed is Earth's radiation. The emittance value is selected first because in WCC the absorptance has a minimal impact due to the Earth's relatively weak radiation. The curves in Fig. 3.3a represent WCC over surface absorbance for various emittance values. This plot indicates that an

emittance of approximately 0.135 is ideal for a preliminary analysis since the WCC temperature always lies between -5°C and 5°C, and the ideal 0°C occurs near the center of the absorptance range. To achieve the ideal WCH temperature 45°C with an emittance of 0.135, the absorptance must be approximately 0.10 as illustrated in Fig. 3.3b.

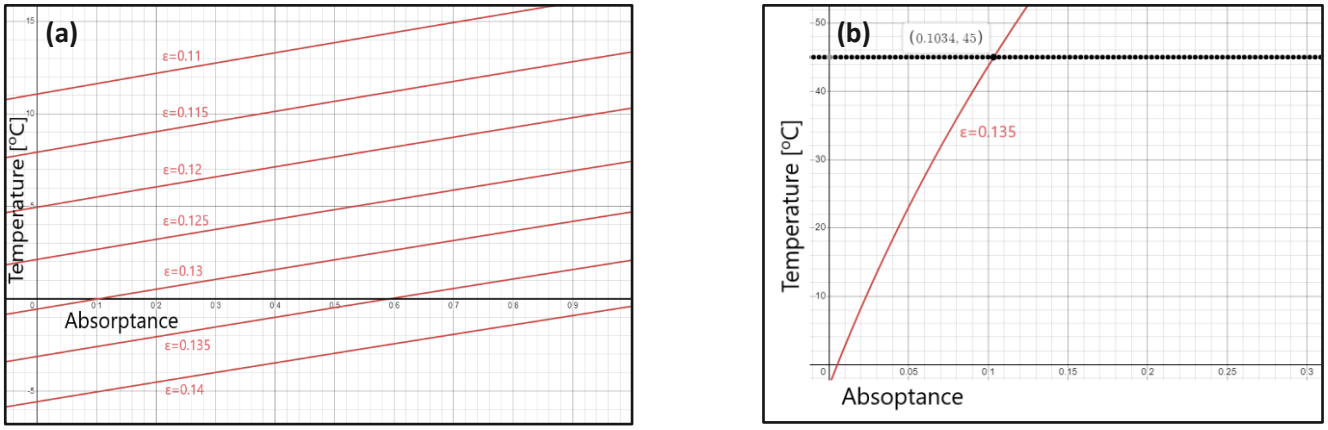

Figure 3.3 – (a) Temperature vs. absorptance at various material emittances during WCC conditions; (b) Temperature vs. absorptance at an emittance of 0.135 during WCH conditions.

Provided the emittance and absorptance values, the sample calculation of Fig. C4 yields a WCC equilibrium surface temperature of -3.93°C. Following a similar approach, when the satellite encounters maximum exposure of the solar irradiance and Earth's albedo, the worst-case hot (WCH) equilibrium surface temperature is 42.89°C. Maximum solar irradiance of 1421 W/m^2 occurs during the winter solstice [9].

To heat the WCC temperature to meet the safety margin of 0°C, around 30W of power is needed. The power budget is adjusted to include thermal subsystem power. Using the revised total power estimate of 471.43W, the surface temperatures of WCC and WCH are -4°C and 45°C respectively. Due to the reduced power dissipated, the material emittance is slightly decreased to a value of 0.1275. A 30W heater is still needed to reach the desired equilibrium temperature including margin (see calculation Fig. C5).

3.6.3 – THERMAL CONTROL MECHANISMS

The surface material of the satellite is aluminum since it can support both the desired emittance and absorptance. Its emittance can be changed easily depending on its surface roughness and oxidization [10].

A resistive heater with an onboard control system will be used to maintain the temperature of the payload within its required operating conditions. Insulating MLI blankets can be used to ensure that the payload is not greatly influenced by the structure's surface temperature. The resistive heater is also implemented to ensure the equilibrium temperature does not drop below the safety limit at 0°C; although this is highly unlikely to happen since it takes time to reach equilibrium and LEO orbits are quick to travel around the globe. These control mechanisms can also account for material degradation towards EOL. If a transient thermal analysis indicates that the temperature of the payload can exceed 21°C, a heat piping mechanism may be introduced.

3.7 – Launch Systems & Propulsion

3.7.1 – LAUNCHER SELECTION

Two launchers have been considered for this mission: the SpaceX Falcon 9 rideshare program, and ESA's Vega rocket. Table 3.4. lists their launch parameters relevant to this preliminary analysis. The launcher selected for this mission is the Falcon 9. The primary reason for this decision is the massively reduced cost. The reduced cost is primarily due to the shared launcher module and the re-useability of the rocket. Vega rockets can also support shared launch modules; however, their payload limit is much smaller, thus incurring greater costs. The launcher also has much more availability and a prestigious reliability track record of successful launches [11].

TABLE 3.4 – Falcon 9 and Vega Launcher Parameters.

Parameter	Falcon 9 Launcher (rideshare) [12]	Vega Launcher (dedicated) [13] [14]
Cost	4.24M $USD	35M – 40M $USD
Altitude (circular)	570 km*	700 km
Inclination	70° *	Any **
Payload Limit	22'800 kg	1500 kg

* Typically 97.6° or 53.2°; however, rideshare with Starlink satellites is available for 70° at 570km if proposed.

** This is implied and to be further discussed once contact with the sales team is established.

3.7.2 – PROPULSION FOR ORBIT INSERTION

The satellite travels from the rocket deployment altitude of 570km to the desired orbital altitude of 830.15km using a Hohmann transfer. The fuel selected for the satellite's thruster is monomethylhydrazine (MMH) which is a commonly used fuel with a specific impulse of 310s [5]. The ΔV needed to enter the transfer orbit is 69.38 m/s and the ΔV needed to exit the transfer orbit at 830.15km is 68.75 m/s. Adding them together yields a total ΔV of 138.13 m/s. Calculations for ΔV and the fuel mass are shown in Fig. C6. The total insertion fuel mass including a 2% residual mass and a 10% margin is approximately 24.87kg. See Table 3.5 for individual fuel component values. As implied by Section 8, no fuel is needed for attitude or orbital maintenance.

TABLE 3.5 – Orbit Insertion Fuel Mass

Fuel Component	Mass [kg]
Minimum Fuel	22.203
Residual (2%)	0.444
Margin (10%)	2.220
TOTAL	24.867

3.7.3 – PROPULSION FOR DE-ORBITING

Following a similar approach to the orbit insertion, a Hohmann transfer is used to de-orbit the satellite at end-of-life. The ΔV needed to enter the transfer orbit is -60.66 m/s and the ΔV needed to exit the transfer orbit at 600km is -53.32 m/s. Adding their magnitudes yields a total ΔV of 113.98 m/s. The total de-orbit fuel mass including a 2% residual mass and a 10% margin is approximately 20.60kg. See Table 3.6 for individual fuel component values.

TABLE 3.6 – De-Orbit Fuel Mass

Fuel Component	Mass [kg]
Minimum Fuel	18.393
Residual (2%)	0.368
Margin (10%)	1.839
TOTAL	20.600

4 – Structures & Configuration

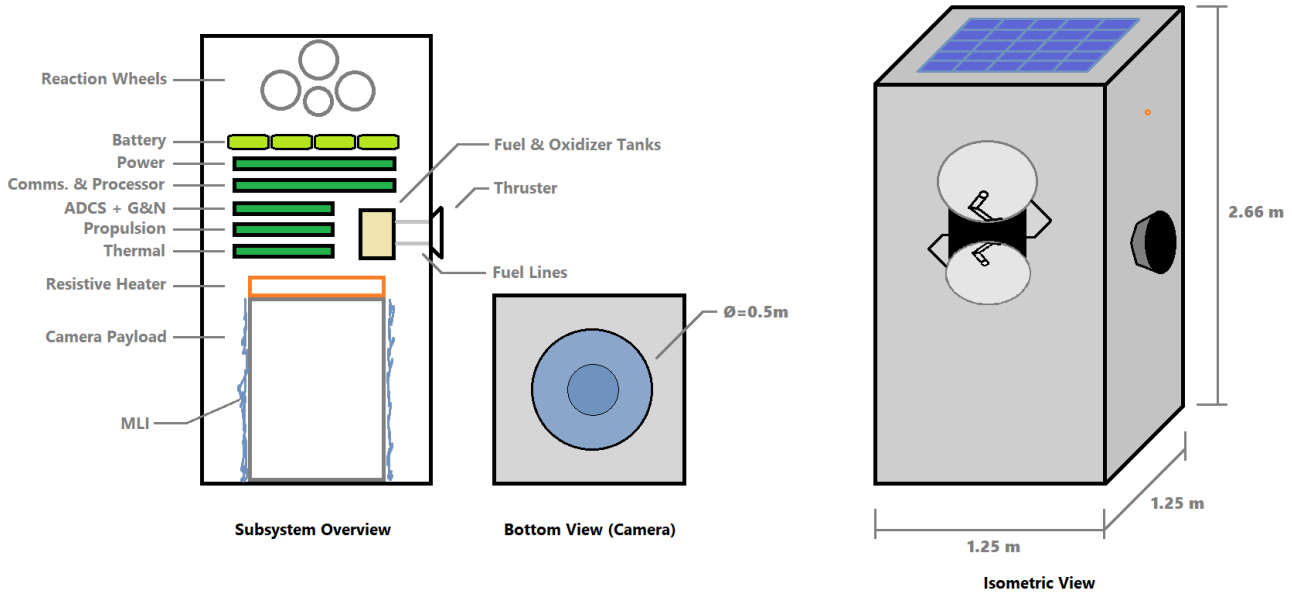

Figure 4.1 – Satellite internal and external structure.

The structure primarily consists of aluminum due to its availability, light weight, and ideal thermal properties as discussed in Section 3.6. See Fig. 4.1 for an illustration of the satellite's internal subsystem placement and external structure. The camera faces outwards of the bottom of the spacecraft. Within the structure, it is coated with MLI and exposed to a resistive heater. Near the resistive heater is the thermal subsystem control circuit. The fuel lines are also placed near the heater to ensure that they don't freeze in space; although unlikely. The thruster is placed on one of the side faces of the satellite to apply a forward or backward impulse in the direction of the orbit. Next to the thruster are the fuel and oxidizer tanks as well as the propulsion subsystem control circuit. The ADCS + G&N, communications, and power boards/circuits are stacked in a modular fashion. The communication board also has a processor used for very basic image compilation to reduce an image to a square shape before transmitting its data. Within the processor there is memory to store images until communications are established with the ground station. At the top of the satellite are the four batteries and four reaction wheels. They are placed on top in an attempt to evenly distribute the mass. The antenna reflector dishes are also placed slightly higher for this reason, as seen in the isometric view. Solar panels are placed on the top side and two of the larger faces of the satellite. To avoid heat distortion and damage, they are not placed near the thruster.

Estimates for the structure's dimensions are calculated in Fig. C7. The total volume and surface area of the satellite is estimated to be $4.17m^3$ and $16.46m^2$ respectively. Of this surface area, $8.21m^2$ is available for solar panels, while only $6.58m^2$ is needed. Edge dimensions are illustrated on Fig. 4.1.

5 – Conclusion

The circular LEO orbit was refined via simulation and has an inclination of 70°, a RAAN of 240°, and a semimajor axis of 7201.15 km. It is possible to further improve the orbit selection by finding a higher orbit that can cover the entire boreal forest in less than 14 days. Consequently, more power would be needed since the image size would be larger and a higher downlink bitrate would be required. It is also possible to optimize the inclination by a few degrees since the camera's FOV is 20° thus it does not need the center line of sight to be at the 70° latitude to observe that part of the forest.

The mass budget estimates a 650kg dry mass including a 30% margin and a 695.5kg wet mass. The initial power budget was revised to account for a resistive heater and a lower downlink transmission cost. The revised power budget boasts a total rating of 471.43W including a 10% margin.

The data budget and data rate analysis are complete and indicate that for the current orbital altitude and inclination a bitrate of 4 Mbps would be sufficient for this mission. The downlink transmit power is -10.28 dBW. Beyond a preliminary design analysis, a more detailed access time will be derived from STK simulations to provide a more accurate bitrate estimate.

The worst-case eclipse time of the satellite is 35.03 minutes which is approximately 34.6% of the orbit. GaAs solar panels with a 244.4 W/m^2 specification during the worst-case scenario were selected. Their mass totaled 37.5 kg, covering nearly 66% of space made available to them on the surface of the satellite. Solar panels on side faces may be tilted slightly to maximize the solar view factor. Lithium-ion batteries were selected for this mission with a total charge capacity of 287.79Wh. They offer a significant advantage over conventional NiCd batteries in terms of rechargeability. Further analyses need to be performed to understand the effectiveness of having batteries that only charge up to 80% and discharge down to 20% to maintain rechargeability health. The satellite uses an unregulated 24V bus and has 10kg of power harness that are estimated to incur up to 5% of losses. A quasi-regulated bus may be used if the unregulated bus proves not ideal for the sensitive payload. In that case, the bus' voltage is regulated during operation under sunlight [5].

Attitude control uses three reaction wheels and a magnetorquer to orient the spacecraft. A fourth reaction wheel is included for redundancy. Gyroscopes and sun sensors are used to determine and calibrate the orientation during the mission. Orbital maneuvers are also needed to insert the satellite into its mission orbit and to de-orbit the satellite at its end-of-life. A propulsion system with 45.47kg of monomethylhydrazine propellant is implemented to perform such orbital maneuvers. The total ΔV needed to move from the launch orbit to the mission orbit is 138.14 m/s while the total ΔV needed to de-orbit the spacecraft is 113.98 m/s. A SpaceX Falcon 9 launcher is used to reach the launch orbit with an altitude of 570km at an inclination of 70°. SpaceX's rideshare program is the most cost-effective solution for this mission.

The thermal subsystem uses material engineering and MLI to passively maintain the surface temperature between -5°C-50°C and the payload temperature between 19°C-21°C. A small 30W resistive heater is included to ensure that the safety margins are not breached. To know whether equilibrium temperatures are reached and at what rate heat transfer occurs, a transient analysis is needed. It is beyond the scope of this preliminary design analysis. Experimental data indicates that a black paint surface finish with an absorptance of 0.9 and an emittance of 0.9 which are far from the specified 0.1 and 0.125 yield equilibrium temperatures between 20°C and -2°C in LEO orbits [5, p. 365]; hence it is clear that this basic preliminary analysis is not acceptable.

Appendix A – Project Schedule

TABLE A1 – Top-level Project Schedule

Phase Name	Phase 0	Phase A	Phase B	Phase C	Phase D	Phase F	Phase E	Phase F
Description	Mission Definition	System Definition	Preliminary Design	Detailed Design	Manufacturing, AI&T	Launch	Operation	Disposal
Year	--	Year 1: Q1	Year 1: Q2	Year 1: Q1&2, Year 2	Year 3	Year 3 End	5 Years	25 Years

The project schedule is similar to the standard schedule defined by the CSA [15]. In Table A1, "Q" represents "Quarter" and "H" represents "Half".

Appendix B – Cost Estimate

TABLE B1 – Mission Cost Breakdown

	Cost [Millions $USD]	Percent
Spacecraft	59.36	70%
AI&T	3.50	4.13%
Launch	4.24	5%
Insurance	0.10	0.12%
Operation	10	10%
Other Fees	7.6	8.96%
TOTAL	84.8	

FireSat had a similar mission and orbit to this satellite. The AI&T costs of FireSat were approximately 3.5M $USD and is assumed to be the AI&T costs of this satellite. The launch cost explored in Section 3.7.1 is 4.24M $USD. The cost of the payload must be requested from the customer. Assuming the launch is 5% of the cost due to the cheaper rideshare service used, the total mission cost is 84.8M $USD. Typically a launch is 20% of the cost and the satellite accounts for 70% of the cost [5]. SpaceX offers insurance up to 2M $USD for 100K $USD. A cost breakdown is available in Table B1.

Appendix C – Calculations

Eclipse Angle

$$\sin\alpha = \frac{R_E}{R_E+H}$$

$$\alpha = \sin^{-1}\frac{R_E}{R_E+H}$$

$$= \sin^{-1}\frac{6371}{6371+830.15} = 1.0859 \text{ rad}$$

Eclipse Time

$$T_e = 2\alpha \times \frac{T}{2\pi}$$

$$= 2(1.0859)\frac{6081.546}{2\pi} = 2102.09\ s\ =\ 35.035\ min$$

Figure C1 – Eclipse time solution process and results.

Beginning-of-Life (BOL)

Assumptions [4]

Ideal Power Density: $PD_0 = 244.4$ W/m²

Inherent Degradation: $I_d = 0.77$

Worst Angle of Incidence: $\theta = 23.5^o$

Calculation

$$PD_{BOL} = PD_0 I_d \cos\theta$$

$$= 244.4 \times 0.77 \times \sin 23.5^o = 172.57 \text{ W/m}^2$$

End-of-Life (EOL)

Assumptions [4]

Degradation /yr: $\eta_d = 0.0375$

Calculation

$$PD_{EOL} = PD_{BOL}(1-\eta_d)^{yrs}$$

$$= 172.57(1-0.0375)^5 = 142.55 \text{ W/m}^2$$

Figure C2 – GaAs solar array power density for BOL and EOL at worst-case solar irradiance.

Battery Charge

Parameters

Number of Batteries: N = 4

Load Power (eclipse): P_e = 471.43 W

Eclipse Time: T_e = 0.5839 hr

Assumptions [4]

Transmission Effectiveness: $\eta = 1.15$

Calculation

$$C_{batt} = n\frac{P_e T_e}{DOD \cdot N}$$

$$= 1.15\frac{471.43(0.5839)}{0.25(4)} = 316.57 \text{ Wh}$$

Figure C3 – Li-Ion battery charge calculation.

Worst Case Cold

$$G_s\frac{A_{sc}}{4}\alpha_s + \dot{q}_E \sin^2(\rho)\, A_{sc}\frac{1-cos\,\rho}{2}\varepsilon_{IR} + G_s A_{sc} a\alpha_s \frac{1-cos\,\rho}{2}\sin^2(\rho) + \dot{Q}_W = \varepsilon_{IR} A_{sc}\sigma T^4$$

(0 over $G_s\frac{A_{sc}}{4}\alpha_s$; 0 over $G_s A_{sc} a\alpha_s \frac{1-cos\,\rho}{2}\sin^2(\rho)$)

$$\dot{q}_E \sin^2(\rho)\, A_{sc}\frac{1-cos\,\rho}{2}\varepsilon_{IR} + \dot{Q}_W = \varepsilon_{IR} A_{sc}\sigma T^4$$

$$(216)\sin^2(0.4849)\,(12.53)\frac{1-cos\,0.4849}{2}(0.9) + 500 = 0.9(12.53)(5.67\times10^{-8})T^4$$

$$T = 269.22\ ^oK = -3.93\ ^oC$$

Figure C4 – Worst case cold surface temperature calculations from the thermal balance equation.

Heater Power @ WCC

ε = 0.1275 $T_{desired}$ = 0°C = 273.15°K T_{WCC} = -4.0066°C = 269.14°K

$$\dot{Q}_{heater} = \varepsilon\sigma\left(T_{desired}^4 - T_{WCC}^4\right) = 0.1275(5.67 \cdot 10^{-8})(273.15^4 - 269.14^4) = 29 \text{ W}$$

Figure C5 – Heater power sample computation.

Initial Orbit [deployment]

$$r_i = H_i + R_E = 6371 + 570 = 6941 \text{ km}$$
$$v_i = \sqrt{\frac{\mu}{r_i}} = \sqrt{\frac{\mu}{6941}} = 7.58 \text{ km/s}$$

Final Orbit [mission]

$$r_f = H_f + R_E = 6371 + 830.15 = 7201.15 \text{ km}$$
$$v_f = \sqrt{\frac{\mu}{r_f}} = \sqrt{\frac{\mu}{7201.15}} = 7.44 \text{ km/s}$$

Transfer Orbit

$$a_t = \frac{r_i + r_f}{2} = \frac{6941 + 7201.15}{2} = 7071.075 \text{ km}$$
$$v_{tp} = \sqrt{\mu\left(\frac{2}{r_i} - \frac{1}{a_t}\right)} = \sqrt{\mu\left(\frac{2}{6941} - \frac{1}{7071}\right)} = 7.65 \text{ km/s}$$
$$v_{ta} = \sqrt{\mu\left(\frac{2}{r_f} - \frac{1}{a_t}\right)} = \sqrt{\mu\left(\frac{2}{7201} - \frac{1}{7071}\right)} = 7.37 \text{ km/s}$$

ΔV Solution

$$\Delta V_1 = v_{tp} - v_i = 7.65 - 7.58 = 0.0694 \text{ km/s}$$
$$\Delta V_2 = v_f - v_{ta} = 7.44 - 7.37 = 0.0687 \text{ km/s}$$
$$\Delta V = |\Delta V_1 + \Delta V_2| = 0.1381 \text{ km/s}$$

Minimum Fuel Mass

I_{sp} = 310s g_0 = 9.81 m/s²

$$m_{fuel} = m_{tot}\left(1 - e^{-\frac{\Delta V}{g_0 I_{sp}}}\right)$$
$$= 500\left(1 - e^{-\frac{138.1}{9.81(310)}}\right) = 22.2026 \text{ kg}$$

Figure C6 – Sample "delta V" and fuel mass computation using the satellite orbit insertion maneuver.

Volume Estimate

$$V = 0.006 \times m_{wet} = 0.006(695.47) \cong 4.17 \text{ m}^2$$

Linear Dimension (Length)

$$L = 0.3 \times m_{wet}^{1/3} = 0.3(695.47)^{\frac{1}{3}} \cong 2.66 \text{ m}$$

Base Area

$$A_{base} = V/L = 4.17/2.66 \cong 1.57 \text{ m}^2$$

Base Dimension (square)

$$x = \sqrt{A_base} = \sqrt{1.57} \cong 1.25 \text{ m}$$

Figure C7 – Satellite dimension estimates.

Appendix D – Geometric Analyses

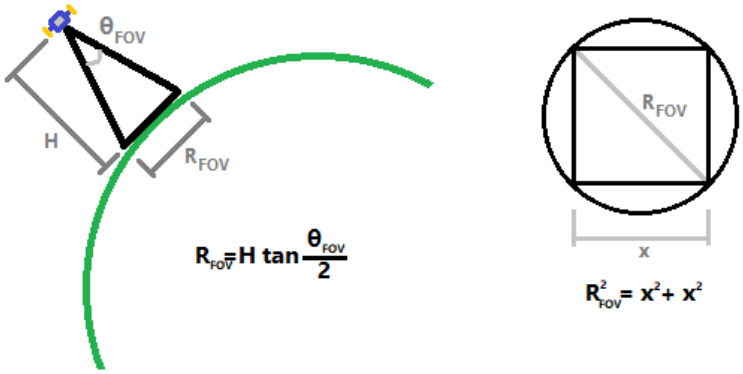

Figure D1 – Geometric overview of the payload's instantaneous ground coverage.

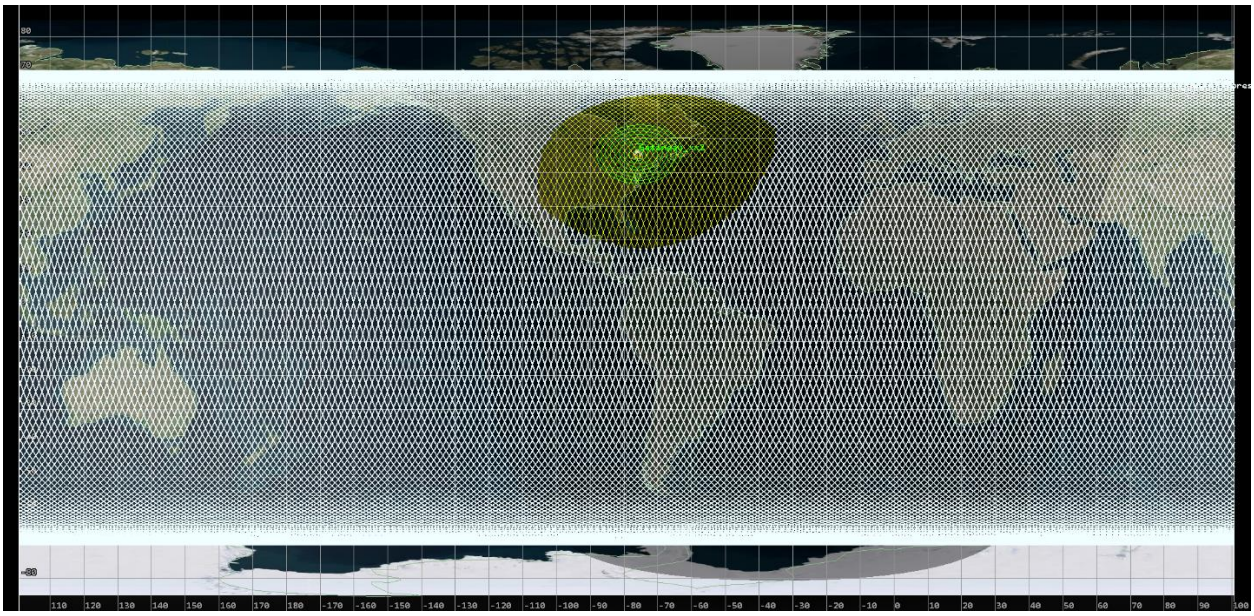

Figure D2 – STK simulated ground tracks.

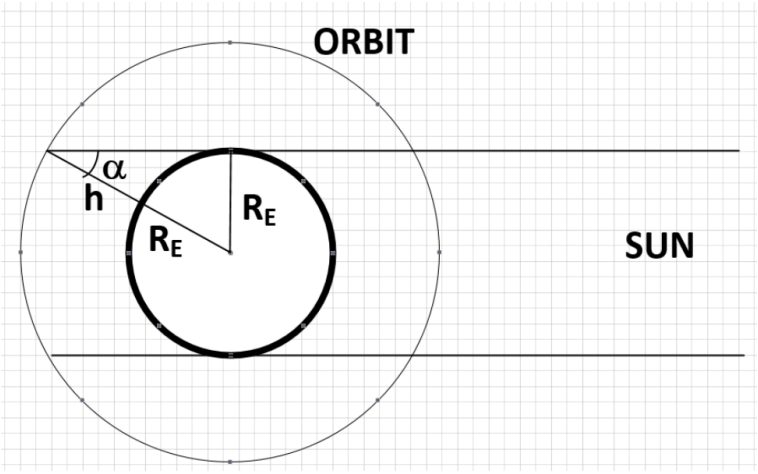

Figure D3 – Geometry of eclipsed region within the Earth's shadow from the sun. [4]

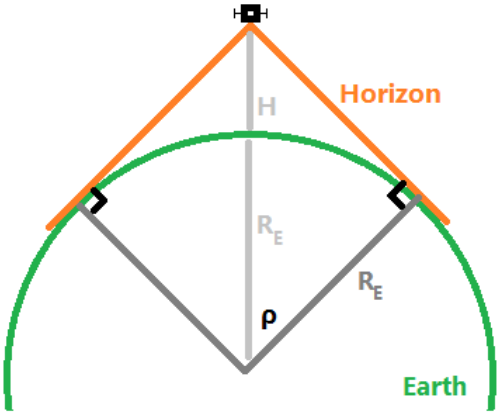

$$\rho = \cos^{-1}\frac{R_E}{R_E + H}$$
$$= \cos^{-1}\frac{6371}{6371 + 830.15}$$
$$= 0.4849 \text{ rad}$$
$$= 27.7829^{o}$$

Figure D4 – Earth angular radius.

References

[1] G. Patrick Juday, "Taiga," *Encyclopedia Britannica*, Apr. 03, 2024. https://www.britannica.com/science/taiga/Trees (accessed Feb. 19, 2024).

[2] K. Bullington, "Radio propagation fundamentals," in *The Bell System Technical Journal*, vol. 36, no. 3, pp. 593-626, May 1957, doi: 10.1002/j.1538-7305.1957.tb03855.x.

[3] "Gatineau Satellite Station." Natural Resources Canada. https://natural-resources.canada.ca/science-data/research-centres-labs/satellite-receiving-stations/satellite-facilities/gatineau-satellite-station/10948 (accessed: 27-Feb-2024).

[4] T. Kaya, "Spacecraft Power Subsystem," lecture presented at Carleton University, Ottawa, ON, February. 2024.

[5] P. Fortescue, G. Swinerd, and J. Stark, *Spacecraft Systems Engineering*. Wiley, 2011.

[6] K. Mallon, F. Assadian, and B. Fu, "Analysis of On-Board photovoltaics for a battery electric bus and their impact on battery lifespan," *Energies*, vol. 10, no. 7, p. 943, Jul. 2017, doi: 10.3390/en10070943.

[7] T. G. R. Reid, "Orbital Diversity for Global Navigation Satellite Systems," PhD thesis, Aeronautics and Astronautics – Stanford University, Stanford, CA, USA, 2017. [Online]. Available: https://www.researchgate.net/publication/323245224_Orbital_Diversity_for_Global_Navigation_Satellite_Systems

[8] T. Kaya, "Spacecraft Guidance and Navigation," lecture presented at Carleton University, Ottawa, ON, March. 2024.

[9] T. Kaya, "Spacecraft Thermal Subsystem," lecture presented at Carleton University, Ottawa, ON, March. 2024.

[10] "Surface emissivity coefficients," *Engineering Toolbox,* Sep. 22, 2023. https://www.engineeringtoolbox.com/emissivity-coefficients-d_447.html

[11] "SpaceX Falcon 9," *SpaceX*. https://www.spacex.com/vehicles/falcon-9/

[12] *Rideshare User's Payload Guide*, 9th ed., SpaceX, Hawthorne, CA, USA, December 2023. https://storage.googleapis.com/rideshare-static/Rideshare_Payload_Users_Guide.pdf

[13] *Vega User's Manual*, 4th Issue, Arianespace Inc., France, April 2014. https://www.arianespace.com/wp-content/uploads/2018/05/Vega-Users-Manual_Issue-04_April-2014.pdf

[14] Arianespace, "Vega - Arianespace," *Arianespace*, Feb. 17, 2021. https://www.arianespace.com/vehicle/vega/

[15] T. Kaya, "Assembly, Integration and Testing (AIT)," lecture presented at Carleton University, Ottawa, ON, March. 2024.

[16] W. J. Larson, J. R. Wertz, and B. D'Souza, *SMAD III: Space Mission Analysis and Design, 3rd Edition : Workbook*. 2005.

AUTHOR'S NOTE: I am a 4th year student, so much of the knowledge, especially in ADCS, is not new to me and I had no need for references. I also would've much rather placed the geometric analysis figures within the report itself; however, I can't exceed the page limit by so much just for that.